BIOLOGY OF REPRODUCTION (2015) **92**(4):102, 1–17
Published online before print 18 March 2015.
DOI 10.1095/biolreprod.114.124388

A Novel Class of Interstitial Cells in the Mouse and Monkey Female Reproductive Tracts[1]

Lauren E. Peri,[3] Byoung H. Koh,[3] Grace K. Ward, Yulia Bayguinov, Sung Jin Hwang, Thomas W. Gould, Catrina J. Mullan, Kenton M. Sanders, and Sean M. Ward[2]

Department of Physiology & Cell Biology, University of Nevada School of Medicine, Reno, Nevada

ABSTRACT

Growing evidence suggests important roles for specialized platelet-derived growth factor receptor alpha-positive (PDGFRalpha$^+$) cells in regulating the behaviors of visceral smooth muscle organs. Examination of the female reproductive tracts of mice and monkeys showed that PDGFRalpha$^+$ cells form extensive networks in ovary, oviduct, and uterus. PDGFRalpha$^+$ cells were located in discrete locations within these organs, and their distribution and density were similar in rodents and primates. PDGFRalpha$^+$ cells were distinct from smooth muscle cells and interstitial cells of Cajal (ICC). This was demonstrated with immunohistochemical techniques and by performing molecular expression studies on PDGFRalpha$^+$ cells from mice with enhanced green fluorescent protein driven off of the endogenous promoter for *Pdgfralpha*. Significant differences in gene expression were found in PDGFRalpha$^+$ cells from ovary, oviduct, and uterus. Differences in gene expression were also detected in cells from different tissue regions within the same organ (e.g., uterine myometrium vs. endometrium). PDGFRalpha$^+$ cells are unlikely to provide pacemaker activity because they lack significant expression of key pacemaker genes found in ICC (*Kit* and *Ano1*). *Gja1* encoding connexin 43 was expressed at relatively high levels in PDGFRalpha$^+$ cells (except in the ovary), suggesting these cells can form gap junctions to one another and neighboring smooth muscle cells. PDGFRalpha$^+$ cells also expressed the early response transcription factor and proto-oncogene *Fos,* particularly in the ovary. These data demonstrate extensive distribution of PDGFRalpha$^+$ cells throughout the female reproductive tract. These cells are a heterogeneous population of cells that are likely to contribute to different aspects of physiological regulation in the various anatomical niches they occupy.

fibroblast-like cells, interstitial cells, PDGFRα^+ cells

INTRODUCTION

The organs of the female reproductive tract provide a diverse array of biological functions, including: 1) growth and maturation of oocytes in the ovary [1–3], 2) transport of mature eggs along the oviduct to the site of fertilization, 3) transport of fertilized embryos through the terminal regions of the duct and into the uterus for implantation [4, 5], 4) development of the fetus within the protective environment of the uterus [6], and 5) expulsion of the fetus through the birth canal [7–9]. Such complicated movements require the coordinated activity of many types of cells, including several types of smooth muscle cells (SMCs), intramural neurons, and specialized interstitial cells providing pacemaker activity (interstitial cells of Cajal [ICCs]) [10].

A population of interstitial cells in the gastrointestinal (GI) tract, known traditionally as fibroblast-like cells [11], has recently been shown to be labeled selectively with antibodies against platelet-derived growth factor receptor α (PDGFRα) [12–14]. Interstitial cells immunopositive for PDGFRα have also been discovered in the muscularis of the bladder [15–17]. PDGFRα^+ cells are distinct from nerve elements, ICCs, and SMCs [12–14]. PDGFRα^+ cells form close associations with nerve fibers, express signal transduction and effector molecules appropriate for receiving and translating neural inputs, and form gap junctions with SMCs. Evidence has developed that PPDGFRα^+ cells in the GI tract and bladder mediate inhibitory neurotransmission in these organs. A second population of PDGFRα^+ cells was also found within the mucosa tissue of mouse and human GI organs [18]. These cells line the epithelium and are closely associated with the basolateral surface of epithelial cells. In the bladder, PDGFRα^+ cells are located in the suburothelium and in the lamina propria of the mucosa [15, 17].

In the present study we have examined the distribution of PDGFRα^+ cells in the mouse and monkey ovary, oviduct, and uterus (endometrium and myometrium). We have found that this class of interstitial cells is extensively distributed throughout the female reproductive tract. Double-labeling immunohistochemistry shows that PDGFRα^+ cells are distinct from SMCs. We also used transgenic mice engineered to express an enhanced green fluorescent protein (eGFP)-histone 2B fusion protein driven off of the endogenous promoter for *Pdgfra* [19]. With these mice we were able to unequivocally identify PDGFRα^+ cells in the mixed cell population after enzymatic dispersion of tissues, sort cells by fluorescence-activated cell sorting (FACS), and perform molecular expression studies to characterize prominent gene expression profiles in order to begin selective phenotyping. We found marked differences in gene expression in PDGFRα^+ cells from the ovary, oviduct, and uterus. This population of cells also showed expression differences within the same organ (e.g., uterine myometrium vs. endometrium). The extensive distribution and differential gene expression profiles of PDGFRα^+

[1]Supported by National Institutes of Health (NIH) grants R01 DK-57326 to S.M.W., R01 DK-091336 to K.M.S. and S.M.W., and GM103554 to T.W.G. Morphological and molecular studies were performed in a Core laboratory supported by NIH grant P01 DK41315. Confocal images were collected using a Zeiss LSM510 Meta confocal microscope obtained with support from the grant NIH1 S10 RR16871. FACS was performed with support from NIH COBRE P30GM110767.

[2]Correspondence: E-mail: smward@medicine.nevada.edu.
[3]These authors contributed equally to this work and should be considered co-first authors.

Received: 27 August 2014.
First decision: 24 September 2014.
Accepted: 12 March 2015.

eISSN: 1529-7268 http://www.biolreprod.org
ISSN: 0006-3363

TABLE 1. Details of primary antibodies used (single or combination).[a]

Antibody[b]	Resource	Monoclonal or polyclonal antibody	Host	Dilution
1. PDGFRα (anti-mouse)	R&D Systems Inc., Minneapolis, MN	Poly	Goat	1:100
2. PDGFRα (anti-mouse)	Affymetrix eBioscience, San Diego, CA	Mono	Rat	1:100
3. PDGFRα (anti-human)	R&D Systems Inc., Minneapolis, MN	Poly	Goat	1:100
4. Smmhc	Biomedical Technologies Inc., Ward Hill, MA	Poly	Rabbit	1:200
5. Vimentin (Syn peptide, Arg28; clone R28)	Cell Signaling Technology, Danvers, MA	Poly	Rabbit	1:100
6. mSCFR (c-Kit; anti-mouse)	R&D Systems Inc., Minneapolis, MN	Poly	Goat	1:500
7. hSCFR (c-Kit); anti-human)	R&D Systems Inc., Minneapolis, MN	Poly	Goat	1:500
8. hSCFR (c-Kit)	PharMingen International, Sparks, MD	Mono	Mouse	1:200
9. CD117 (c-Kit; anti-mouse)	eBiosciences, San Diego, CA	Mono	Rate	1:200

[a] For double-labeling experiments, the following antibody combinations were used: mouse = PDGFRα/Smmhc: 1&4, PDGFRα/vimentin: 1&5, PDGFRα/c-Kit: 1 2 monkey = PDGFRα/Smmhc: 3&4, PDGFRα/vimentin: 3&5, PDGFRα/c-Kit: 3&8.
[b] SCFR: anti-stem cell factor receptor (Kit).

cells throughout the female reproductive tract suggest this population of interstitial cells has multiple and region-specific physiological roles.

MATERIALS AND METHODS

Animals

Female *Pdgfra*$^{tm11\ (EGFP)Sor}$/J and C57BL/6 mice were obtained from The Jackson Laboratory. Mice were exposed to isoflurane (AErrane; Baxter) inhalation, immediately followed by cervical dislocation. An incision was made in the abdominal wall, and the ovaries, oviducts, and uterine horns were removed and placed in Krebs-Ringer buffer (mmol L^{-1}): NaCl, 118.5; KCl, 4.5; $MgCl_2$, 1.2; $NaHCO_3$, 23.8; KH_2PO_4, 1.2; dextrose, 11.0; and $CaCl_2$, 2.4, at 4°C for further preparation. Reproductive tissues were collected from mice during the proestrus stage of the estrus cycle, which was determined by cytological analysis of vaginal smears. The Institutional Animal Care and Use Committee at the University of Nevada, Reno approved all procedures used. The female reproductive tracts from cynomolgus monkeys between the ages of 2 and 8 yr were obtained from Charles River Laboratories and used for the studies described. Tissues were transported in precooled Krebs-Ringer buffer to the University of Nevada, Reno and fixed within 2 h after animals were killed. All animals were maintained and experiments performed in accordance with the National Institutes of Health Guide for the Care and Use of Laboratory Animals.

TABLE 2. Details of primers used for molecular studies.

Primer name	Primer sequence	Accession no.
Gapdh-F	TGAACGGATTTGGCCGTATTG	NM_008084
Gapdh-R	GATGGGCTTCCCGTTGATGA	
Pdgfra-F	ATGACAGCAGGCAGGGCTTCAACG	NM_011058
Pdgfra-R	CGGCACAGGTCACCACGATCGTTT	
Myh11-F	CTACACTGCGCAATACCACG	NM_013607
Myh11-R	TGCCAGGATCTCATAGCGTT	
Kit-F	CGCCTGCCGAAATGTATGACG	NM_021099
Kit-R	GGTTCTCTGGGTTGGGGTTGC	
Vim-F	GCGAGAGAAATTGCAGGAGG	NM_011701
Vim-R	CCGTTCAAGGTCAAGACGTG	
Cd34-F	CTAGTGTCTGCTCCCTGCTT	NM_133654
Cd34-R	TTCGGGAATAGCTCTGGTGG	
Gja1-F	GAAGTTCAAGTATGGGATTGAAGAACACG	NM_010288
Gja1-R	GGGATCTCTCTTGCAGGTGTAGAC	
Cd44-F	ATGGCCGCTACAGTATCTCC	NM_009851
Cd44-R	GCACAGATAGCGTTGGGATG	
Ano1-F	TAACCCTGCCACCGTCTTCT	NM_178642
Ano1-R	ATGATCCTTGACAGCTTCCTCC	
P2ry1-F	TGACTGGATCTTCGGGGATG	NM_008772
P2ry1-R	ACTTGAGAGGGTACACCACG	
Kcnn3-F	CTGCTGGTGTTCAGCATCTCTCTG	NM_080466
Kcnn3-R	GTCCCCATAGCCAATGGAAAGGAAC	
Fos-F	TTCCTGGCAATAGCGTGTTC	NM_010234
Fos-R	ACCACCTCGACAATGCATGA	

Immunohistochemistry

Mouse female reproductive tracts were pinned to the base of a Sylgard elastomer-lined (Dow Corning), and ovaries and oviducts were isolated from uterine horns by sharp dissection. Oviducts were uncoiled by microdissection from the ''proper ligament'' and pinned to the Sylgard base so that the ampulla-to-isthmus orientation was retained for future identification. In nonhuman primate (NHP) tissues, ovaries and oviducts were separated from uterus as described above. Tissues were fixed in paraformaldehyde (4% w/v in 0.1 M PBS for 15 min at 4°C) or acetone (10 min at 4°C) for mouse tissues, or 1 h (paraformaldehyde) and 30 min (acetone) for monkey. Following fixation, some oviducts were separated into ampulla and isthmus segments for transverse sections, whereas others were kept intact for longitudinal-orientated sections. All tissues were washed for 24 h in PBS (0.01 M, pH 7.2). For cryostat sections tissues were dehydrated in graded sucrose solutions (5%, 10%, 15%, and 20% w/v in PBS; 15 min each for 5%, 10%, and 15%, and overnight in 20%), embedded in a 1:1 mixture of 20% sucrose in PBS and Tissue Tek (Miles), and rapidly frozen in liquid nitrogen-cooled 2-methylbutane. Cryostat sections (10 μm) were cut (Leica CM3050 cryostat) and collected on Vectabond-coated slides (Vector Labs Inc.). Sections were washed in PBS (4 × 15 min) and incubated with bovine serum albumin (1% w/v; Sigma Chemical Co.) for 1 h at room temperature. Primary and secondary antibody combinations and concentrations used are listed in Table 1. Immunoreactivity was detected using the appropriate Alexa Fluor 488 or 594 secondary antibodies (Life Technologies). Before mounting, tissue sections were washed overnight in 0.01 M PBS to remove excess secondary antibody. Control experiments were performed in the absence of primary or secondary antibodies. Mounted specimens were examined using a Zeiss LSM 510 Meta confocal microscope (Carl Zeiss). Confocal micrographs are digital composites of Z-series scans of 1-μm optical sections. Final 1-μm images were constructed, and montages were assembled using a Zeiss LSM 5 Image Examiner and converted to Tiff files for final processing in Adobe Photoshop CS5 software (Adobe Co.) and Photoshop 7.0 and Corel Draw 7.0 (Corel Corp.).

Tissue Dispersion and Cell Purification

Mouse ovaries, oviducts, and uterine horns were equilibrated in Ca^{2+}-free Hanks solution, tissues were dissected into 1 mm^3, and cells were enzymatically dispersed as described previously [20]. Following enzymatic dispersion cells were immediately suspended in Hanks solution at 4°C to minimize gene transcript changes. The $eGFP^+$-PDGFRα cells were purified by FACS (Becton Dickinson FACSAriaII) using the blue laser (488 nm) and eGFP emission detector (530/30 nm). Expression of genes in $PDGFR\alpha^+$ cells was compared against expression in the total cell population from each organ. Total cell population represents all cells dispersed from each organ ($eGFP^+$ and $eGFP^-$).

RNA Isolation and Quantitative RT-PCR

Total RNA was isolated from $PDGFR\alpha^+$ cells from ovaries, oviducts, and uterus using an illustra RNAspin Mini RNA Isolation kit (GE Healthcare). Concentration and purity of RNA were measured using an ND-1000 Nanodrop Spectrophotometer (Nanodrop). Total RNA was reverse transcribed with qScript cDNA SuperMix (Quanta Biosciences) in a 5× reaction buffer containing optimized concentrations of $MgCl_2$, deoxynucleoside triphosphates (deoxyadenosine triphosphate, deoxycytidine triphosphate, deoxyguanosine triphosphate, and deoxythymidine triphosphate), recombinant RNase inhibitor

protein, qScript reverse transcriptase, random primers, oligo (dT) primer, and stabilizers, followed by heat inactivation. Polymerase chain reaction was performed with specific primers (Table 2) using Go-Taq Green Master Mix (Promega Corp.) for 30 cycles of 95°C for 15 sec, 60°C for 30 sec, and 72°C for 30 sec. The PCR products were analyzed on 2% agarose gels and visualized by ethidium bromide. Quantitative RT-PCR was performed with the same primers as PCR using Fast Sybr green chemistry on the 7900HT Real Time PCR System (Applied Biosystems). Cell populations from each organ were prepared from three mice. Normalized values and SDs were calculated in differences of relative gene expression from four dilutions of technical duplicates of reproductive organs from each animal. The data are shown as averages and SDs of triplicate samples (n = 3). Genes with a fold change *P* value less than 0.05 between sorted PDGFRα^+ and unsorted cells represent a statistically significant difference. Unpaired Student *t*-test was used to determine *P* values in the parametric analysis.

RESULTS

Enhanced GFP PDGFRα^+ Cells Within the Mouse Female Reproductive Tract

The distribution of PDGFRα^+ cells in the murine female reproductive tract was examined using *Pdgfr$\alpha^{tm11\ (EGFP)Sor}$*/J mice. Because eGFP is expressed in these mice as a fusion protein with histone 2B, it is limited to cell nuclei [19]. Therefore, we used fluorescence in combination with differential interference contrast (DIC) microscopy to identify the structures of the different reproductive organs and reveal the distribution of PDGFRα^+ cells. We also verified that cells expressing eGFP were PDGFRα^+ cells by double labeling of cells with PDGFRα antibodies (see below).

In the ovaries, PDGFRα^+ cells were distributed within the theca externa and interna (Fig. 1, A–F). PDGFRα^+ cells surrounded follicles (Fig. 1, B and E). Granulosa cells were also PDGFRα^+ (Fig. 1, E and F). At higher magnification, the ovarian surface epithelium surrounding the ovaries was also found to contain PDGFRα^+ cells (Fig. 1, A–F). The distribution of PDGFRα^+ cells in oviducts depended on the region of the oviduct. In the ampulla, PDGFRα^+ cells were found within the myosalpinx and endosalpinx. In the mucosa, PDGFRα^+ cells were located in folds deep into the lumen of the duct (Fig. 1, G–I). In the isthmus, PDGFRα^+ cells were located in the thicker myosalpinx and also in the epithelium (Fig. 1, J–L). Because the mucosal folds are not as prominent in the isthmus as in the ampulla, PDGFRα^+ cells were not as numerous in this location. In the uterine horn, eGFP$^+$ nuclei were densely distributed throughout the myometrium and within the stroma of the endometrium (Fig. 1, M–O).

The cytoplasmic processes and general morphology of PDGFRα^+ cells were investigated by secondary labeling of cells expressing eGFP with antibodies against PDGFRα. Immunolabeling of cells in the ovaries of mice identified an extensive network of PDGFRα^+ cells (Fig. 2). PDGFRα immunoreactivity was broadly distributed within the stroma, theca interna and externa, and ovarian epithelium (Fig. 2, A–F). Enhanced GFP$^+$ nuclei were located within cells immunopositive for PDGFRα. The processes of the PDGFRα^+ cells were intertwined with adjacent PDGFRα^+ cells, making it difficult to identify individual cellular structures (Fig. 2, G–I).

PDGFRα^+ cells were distributed along the outer periphery of oviducts and within the myosalpinx (Fig. 3, A–I). A dense distribution of PDGFRα^+ cells was also observed along the inner aspect representing the mucosal epithelium (Fig. 3, A–F and J–L). In the ampulla region, PDGFRα^+ cells were detected deep within the endosalpinx folds, whereas in the isthmus region the cells were distributed within the epithelial stroma along the inner aspect of the myosalpinx (Fig. 3, D–I).

In the uterus, PDGFRα^+ cells formed a dense network in the endometrial stroma that extended from the myometrial edge to the innermost epithelial lining (Fig. 4). PDGFRα^+ cells were also extensively distributed within the myometrium, where they formed a network from the inner endometrial/myometrial surface to the serosal edge (Fig. 4, G–I).

Previously, studies have reported that some SMCs express PDGFRα, either during development or as a mature phenotype [21, 22]. We investigated whether PDGFRα^+ cells are a cell type distinct from SMCs in the reproductive tract by performing double labeling with antibodies against PDGFRα and smooth muscle myosin II heavy chain (Smmhc), a specific marker for SMCs. In the ovary, PDGFRα^+ cells were a distinct population of cells from SMCs (Fig. 5, A–C). Smmhc$^+$ cells were sandwiched between an inner and an outer layer of PDGFRα^+ cells. A novel observation in these experiments was the presence of a very distinct SMC layer, several cells in thickness, surrounded by maturing follicles (Fig. 5, A–C). In some sections there was an apparent thinning of the smooth muscle layer towards the outer edges of the larger follicles, suggesting the possible involvement of smooth muscle contraction and an asymmetric contractile force that could rupture at this thinner site during ovulation, allowing for the release of the egg (Fig. 5, A–C) [23–25].

Double labeling of the ampulla and isthmus of oviducts with antibodies against PDGFRα and Smmhc showed that PDGFRα^+ cells are also distinct from SMCs along the length of the oviduct (Fig. 5, D–I). In the ampulla, PDGFRα^+ cells were located along the serosa of the ducts and were tightly interspersed with SMCs in the myosalpinx. PDGFRα^+ cells extended deeper into the lamina propria of the endosalpinx than the Smmhc$^+$ SMCs (Fig. 5, D–F). In the isthmus, PDGFRα^+ cells were present in similar locations as have been described for the ampulla region but were in higher density, likely because of the thicker muscle wall in this region of the duct (Fig. 5, G–I). Double labeling also confirmed that the Pdgfrα^+ cells were not immunoreactive for the receptor tyrosine kinase Kit, ruling them out as ICCs in the oviduct (data not shown), as previously described [26].

In the uterus, PDGFRα^+ cells were densely distributed in the endometrial stroma, which matched the distribution of eGFP$^+$ nuclei in PDGFRα cells shown in Figure 1, M–O (Fig. 4). PDGFRα immunoreactivity was also observed in the myometrium. This labeling was restricted to the interstitial spaces between SMCs. As in other locations in the female reproductive tract, cellular colocalization of PDGFRα and Smmhc immunoreactivity was not observed (Fig. 5, J–L). A thin layer of PDGFRα^+ cells was also detected on the serosal aspect of the myometrium that matched the eGFP nuclear labeling in this region of the uterine wall (see Fig. 1, M–O, and Fig. 5, J and L).

Organs from the female reproductive tract were also double labeled with antibodies against PDGFRα and vimentin because this is a common label used for the identification of interstitial cells in the GI tract [27] and bladder [15], and *Vim* transcripts were expressed in *Pdgfra*$^+$ cells (see below). Few PDGFRα^+ cells displayed vimentin-like immunoreactivity in the female murine reproductive tract (Fig. 6).

PDGFRα^+ Cells in the NHP Female Reproductive Tract

We also investigated the distribution and density of PDGFRα^+ cells in the female reproductive tract of cymologous monkeys, a widely used primate model that shares approximately 93% DNA sequence homology with humans [28]. In NHP ovaries, PDGFRα^+ cells were widely distributed within the theca externa and interna. The density was similar or

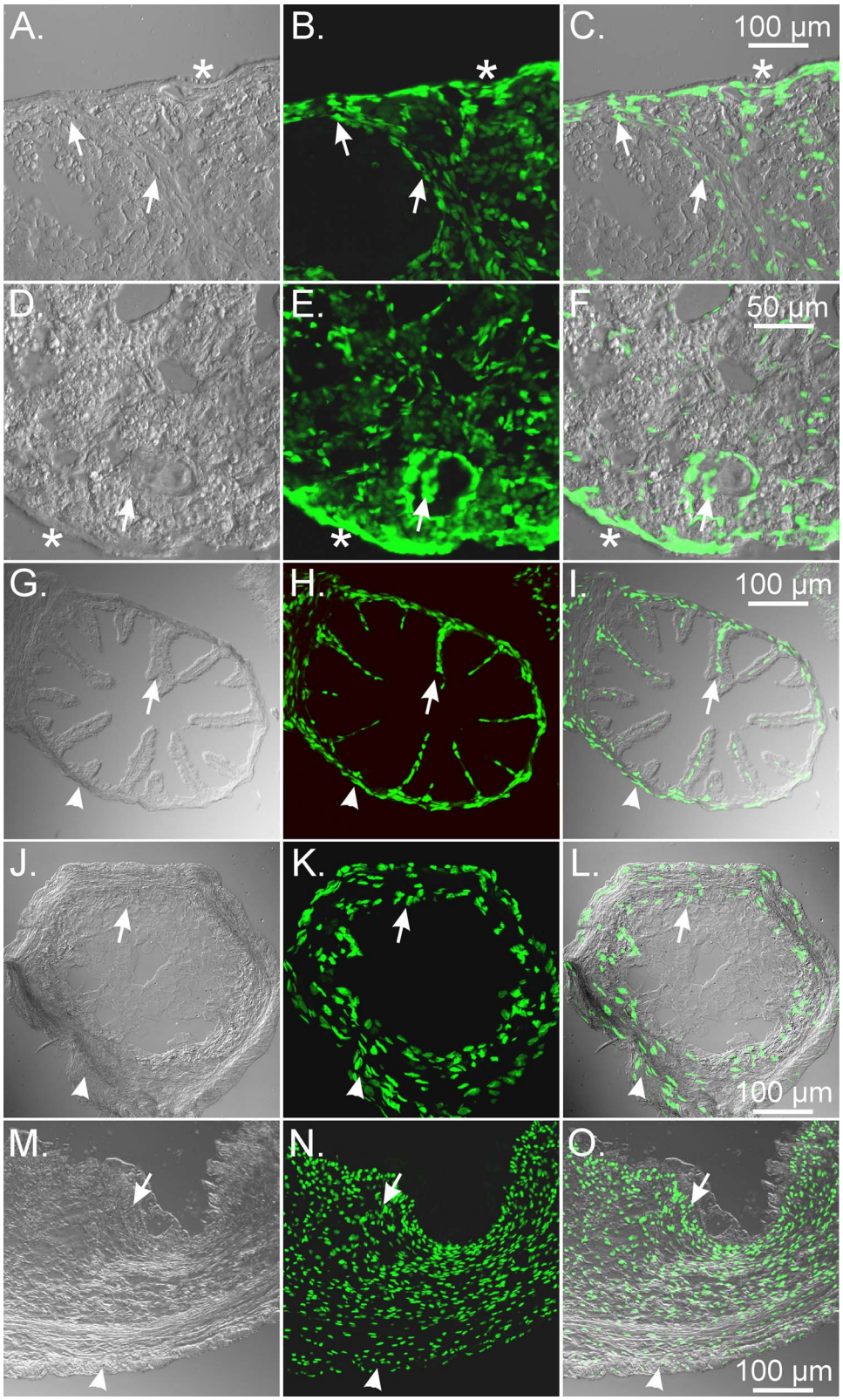

FIG. 1. Distribution of eGFP PDGFRα$^+$ cells in the female reproductive tract of the mouse. Fluorescence microscopy and DIC were used to identify the location of eGFP PDGFRα $^+$ nuclei within the female reproductive tract. **A**–**F**) The eGFP PDGFRα$^+$ nuclei were densely distributed within the ovary stroma and the theca externa and interna. The eGFP PDGFRα$^+$ nuclei were observed to surround follicles (**A**–**C**). Granulosa cells were PDGFRα$^+$ (arrows). The ovarian epithelium also contained PDGFRα$^+$ nuclei (**A**–**F**, asterisks). **G**–**L**) Distribution of eGFP PDGFRα$^+$ nuclei within the oviduct. In the ampulla, eGFP PDGFRα$^+$ nuclei were located within the myosalpinx (**G**–**I**, arrowheads) and were also found within the folds of the endosalpinx (**G**–**I**, arrows). In the isthmus region, eGFP PDGFRα$^+$ nuclei were located within the thicker muscle wall (**J**–**L**, arrowheads) and also in the underlying epithelium (arrows). **M**–**O**) In the uterine horn, eGFP$^+$ nuclei were densely distributed within the myometrium (arrowheads) and within the stroma of the endometrium (arrows). Bars indicated in **C**, **F**, **I**, **L**, and **O** correspond to their respective panels.

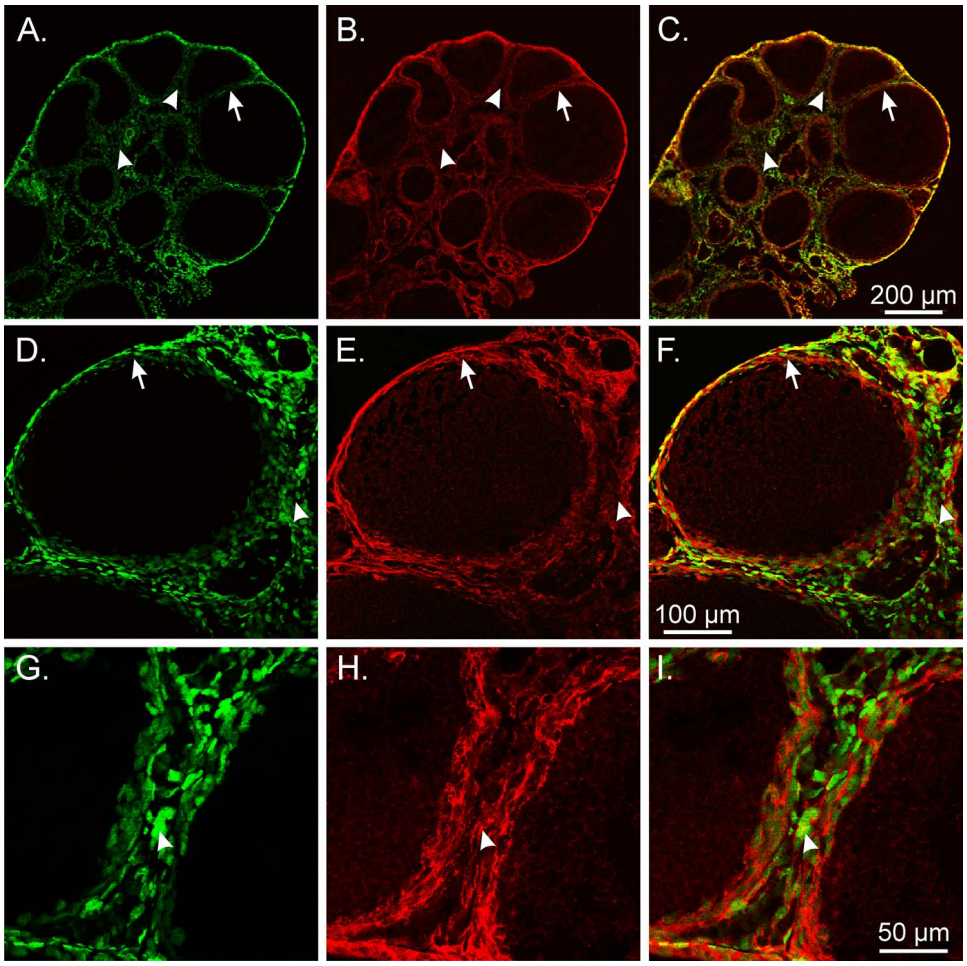

FIG. 2. Double labeling of eGFP PDGFRα^+ nuclei and PDGFRα antibody in the mouse ovary. **A–I**) PDGFRα immunolabeling of mice ovaries identified an extensive network of PDGFRα^+ cells (red) that were distributed within the stroma, theca (arrowheads), and other granulosa cells; around follicles (arrows); and along the ovarian surface epithelium. The eGFP$^+$ nuclei were located within the cell bodies of PDGFRα^+ cells. The processes of PDGFRα^+ interweaved with adjacent PDGFRα^+ cells and other cellular phenotypes that left it difficult to identify individual cellular structures (**G–I**). Bars indicated in **C**, **F**, and **I** and correspond to their respective panels.

possibly greater than that observed in the mouse (Fig. 7). Double labeling with PDGFRα^+ cells and Smmhc revealed that these cells were immunonegative for Smmhc, suggesting that they were a population of cells distinct from SMCs (Fig. 7). Similar to that observed in mouse, there were distinct layers of Smmhc$^+$ SMCs that surrounded follicles and were found on the inner/outer layers of PDGFRα^+ cells that also surrounded follicles, providing evidence that the presence of SMCs around follicles also occurs in primates.

In the NHP oviduct, PDGFRα^+ cells also formed a distinct cellular phenotype from smooth muscle within the myosalpinx and epithelium (Fig. 8, A–F). In the monkey uterus, PDGFRα^+ cells were preferentially located within the interstitial spaces surrounding and between larger smooth muscle bundles. In the myometrium, PDGFRα^+ cells were also found interposed between SMCs within muscle bundles (Fig. 8, G–L), whereas in the endometrium PDGFRα^+ cells were widely distributed in a dense meshwork but were distinct from SMCs that were predominantly located within blood vessels (Fig. 8, M–O).

Nonhuman primate female reproductive tracts were also double labeled with antibodies against PDGFRα and vimentin. Except for the uterine endometrium, only occasional PDGFRα^+ cells displayed vimentin-like immunoreactivity in the monkey female reproductive tract (Fig. 9). These data suggest that vimentin is not a suitable label for the identification of these cells in the female reproductive tract.

Isolation and Molecular Characterization of PDGFRα^+ Cells from the Female Reproductive Tract

PDGFRα^+ cells from *Pdgfra$^{tm11\ (EGFP)Sor}$*/J mice were readily identified in enzymatic dispersions of reproductive organs (Fig. 8, A–L), making it possible to sort these cells by FACS using the fluorescence of eGFP located to the nuclei. We used these techniques to evaluate the expression of genes in the populations of PDGFRα^+ cells isolated from the female reproductive tract and characterized genes encoding receptors and downstream signaling molecules expressed by these cells. Gene expression in PDGFRα^+ cells were compared with total cell expression levels from the tissues where the cells originally resided. Sorting plots of the enriched populations of PDGFRα^+ cells from ovary, oviduct, uterus myometrium, and endometrium are shown (Fig. 10, M–P). Gates on each plot represent the PDGFRα^+ cell population sorted for end point PCR and qPCR analyses.

We characterized the phenotypes of PDGFRα^+ cells from different organs using genes associated with distinct mesenchymal cell groups: 1) SMCs, 2) ICCs, 3) fibroblast-like cells,

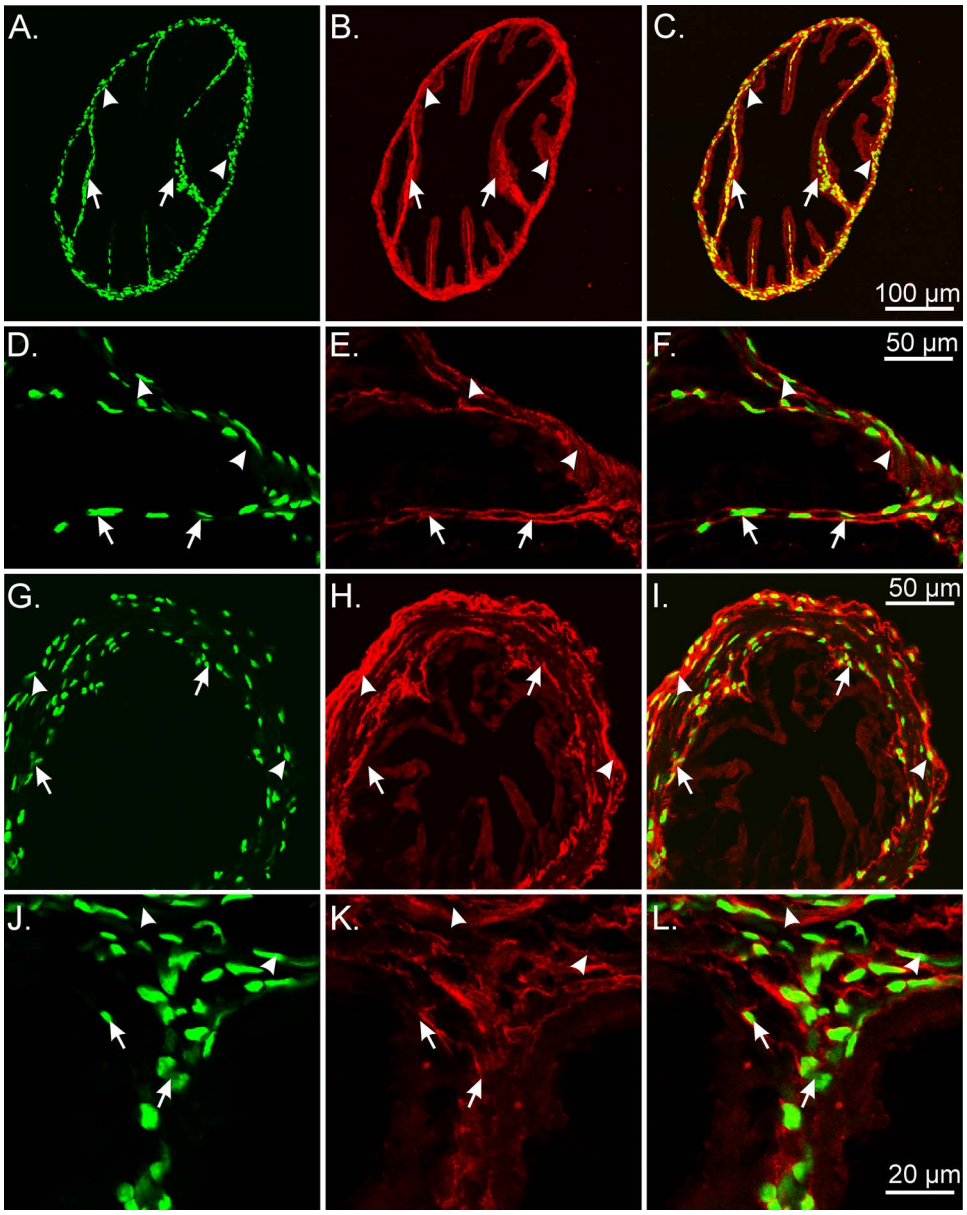

FIG. 3. The eGFP nuclei within PDGFRα$^+$cells in the mouse oviduct. PDGFRα$^+$ cells were densely distributed within the myosalpinx and endosalpinx. The eGFP nuclei (green) were located within the cytoplasm of PDGFRα$^+$ cells (red) throughout the oviduct. **A**–**F**) In the ampulla region, PDGFRα$^+$ cells were detected deep within the endosalpinx folds (arrows), and within the thin-walled myosalpinx (arrowheads). In the isthmus region of the duct (**G**–**I**), PDGFRα$^+$ cells were distributed within the epithelial stroma along the inner aspect of the myosalpinx (arrows; red). The cytoplasm of PDGFRα$^+$ cells was also densely distributed on the outer periphery and more loosely distributed within the myosalpinx (arrows). **J**–**L**) Higher-power images showing the eGFP nuclei within PDGFR$^+$ cells in the myosalpinx (arrowheads) and endosalpinx folds (arrows). Bars in **C**, **F**, **I**, and **L** represent their respective series of panels.

4) myofibroblasts, and 5) mesenchymal stem cells. A secondary analysis was performed using genes indicative of cellular functions. We probed expression of genes involved in 1) housekeeping, 2) pacemaker activity, 3) hormone and neurotransmitter receptors, 4) signal transduction, and 5) proliferation, migration, and connectivity. In confirmation of cell purity, PDGFRα was expressed highly in cells from all organs sorted on eGFP compared with the total cell population (Fig. 11 and Table 3). PDGFRα$^+$ cells did not express a smooth muscle phenotype, because weaker expression of *Myh11* was detected in PDGFRα$^+$ cells from all organs except the ovary, compared with total cellular expression. These data support the immunohistochemical analysis that PDGFRα$^+$ cells are a cellular population distinct from SMCs (Fig. 5). It is unlikely that the PDGFRα$^+$ cells represent a subpopulation of ICCs and are involved in pacemaker activity, because they expressed the prominent ICC gene *Kit* weaker than total cellular expression, and *Ano1* (see below) was almost undetectable. These data were also consistent with the immunohistochemical findings that PDGFRα$^+$ cells represent a population of cells distinct from ICCs. The fibroblast-like or myofibroblast phenotype in ovary PDGFRα$^+$ cells was investigated by probing for *Vimentin* (*Vim*), *Cd34*, and *Gja1* (encoding the gap junction alpha-1 protein or connexin 43). PDGFRα$^+$ cells displayed enhanced *Vim* and *Cd34* compared with the total cell population. However, it is unlikely *Vim* is translated, because of the lack of immunohistochemical detection or protein in these cells in the mouse reproductive

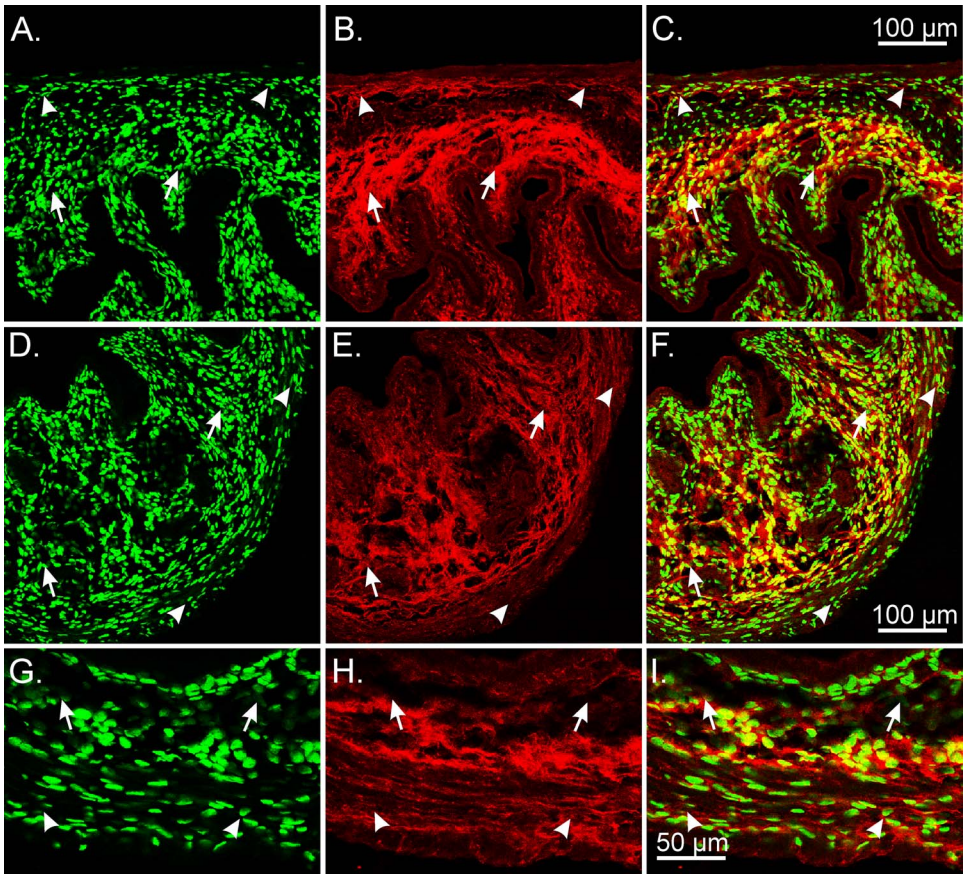

FIG. 4. Identification of eGFP nuclei within PDGFRα$^+$ cells in the mouse uterus. **A**–**F**) PDGFRα immunoreactivity (red) revealed a very dense interconnecting network of cells within the myometrium (arrowheads) and endometrium (arrows). **G**–**I**) At higher magnification, eGFP nuclei were within the cytoplasm of Pdgfrα$^+$ cells. Bars in **C**, **F**, and **I** represent their respective series of panels.

tract. *Gja1* was more highly expressed in PDGFRα$^+$ cells in oviduct and uterine myometrium and endometrium but was downregulated in ovary compared with total cellular expression. *Cd34* and *Cd44* were evaluated to identify possible mesenchymal stem cell gene expression in PDGFRα$^+$ cells. *Cd34* was more highly expressed in PDGFRα$^+$ cells in all organs of the female reproductive tract in comparison with the total cell population, whereas *Cd44* transcripts were enhanced in ovary PDGFRα$^+$ cells, were not different in the oviduct, and were weaker in the uterus (Fig. 11 and Table 3).

An analysis of genes involved in cellular function revealed that *Ano1*—encoding a calcium-activated chloride conductance anoctamin-1, also known as Tmem16a, that is highly expressed in ICCs (see above) and is responsible for the generation of pacemaker activity in the GI tract [20, 29]—was present in oviduct and uterus but not resolved in the PDGFRα$^+$ cells of these organs. The purine receptor *P2ry1* was more highly expressed in PDGFRα$^+$ throughout all organs of the female reproductive tract, as was *Kcnn3*, encoding the apamin-sensitive small conductance calcium-activated potassium channel SK3 or $K_{Ca}2.3$. These two genes are highly expressed in PDGFRα$^+$ cells in the GI tract and bladder, where they are involved in mediating and transducing purine neural or hormonal responses in these tissues. Finally, because of the high density of PDGFRα$^+$ cells throughout the female reproductive tract, we evaluated these cells for expression of the early response transcription factor and proto-oncogene *Fos*. *Fos* was very highly expressed in PDGFRα$^+$ cells in the ovary compared with total cellular expression, was expressed to a lesser degree in uterine myometrium, and was downregulated in the endometrium (Fig. 12 and Table 3). Regional differences in gene expression suggest different physiological functions for PDGFRα$^+$ cells in different organs and in different regions of the same organ of the female reproductive tract (Table 3).

DISCUSSION

In the present study we showed that *Pdgfra$^{tm11\ (EGFP)Sor}$*/J mice provide a powerful new model for studying PDGFRα$^+$ cells, a new class of interstitial cells in the female reproductive tract. Antibodies against PDGFRα verified that the fluorescent eGFP-histone 2B fusion protein is expressed in PDGFRα$^+$ cells with high fidelity. PDGFRα$^+$ cells were shown to be a distinct class of cells in reproductive organs, with very extensive distributions in both muscle and mucosal layers. Cells isolated from tissues of *Pdgfra$^{tm11\ (EGFP)Sor}$*/J mice by enzymatic dispersion can be easily recognized for future molecular and physiological studies. Phenotyping showed an array of genes expressed differentially in PDGFRα$^+$ cells in different organs and regions of organs. The distribution of PDGFRα$^+$ cells in monkeys and mice was remarkably similar, suggesting that mice will be a suitable model for the study of this type of interstitial cells in reproductive organs.

Previously, expressions of PDGFs and PDGFRs in the rat and porcine ovaries have been investigated at different developmental stages and within the corpus luteum of sexually mature adults. The effects of PDGF ligands and receptors on luteogenesis in the rat were also examined [30, 31]. In the rat ovary, PDGF proteins (PdgfA, PdgfB, and PdgfC) were localized to the oocyte membrane or surrounding somatic

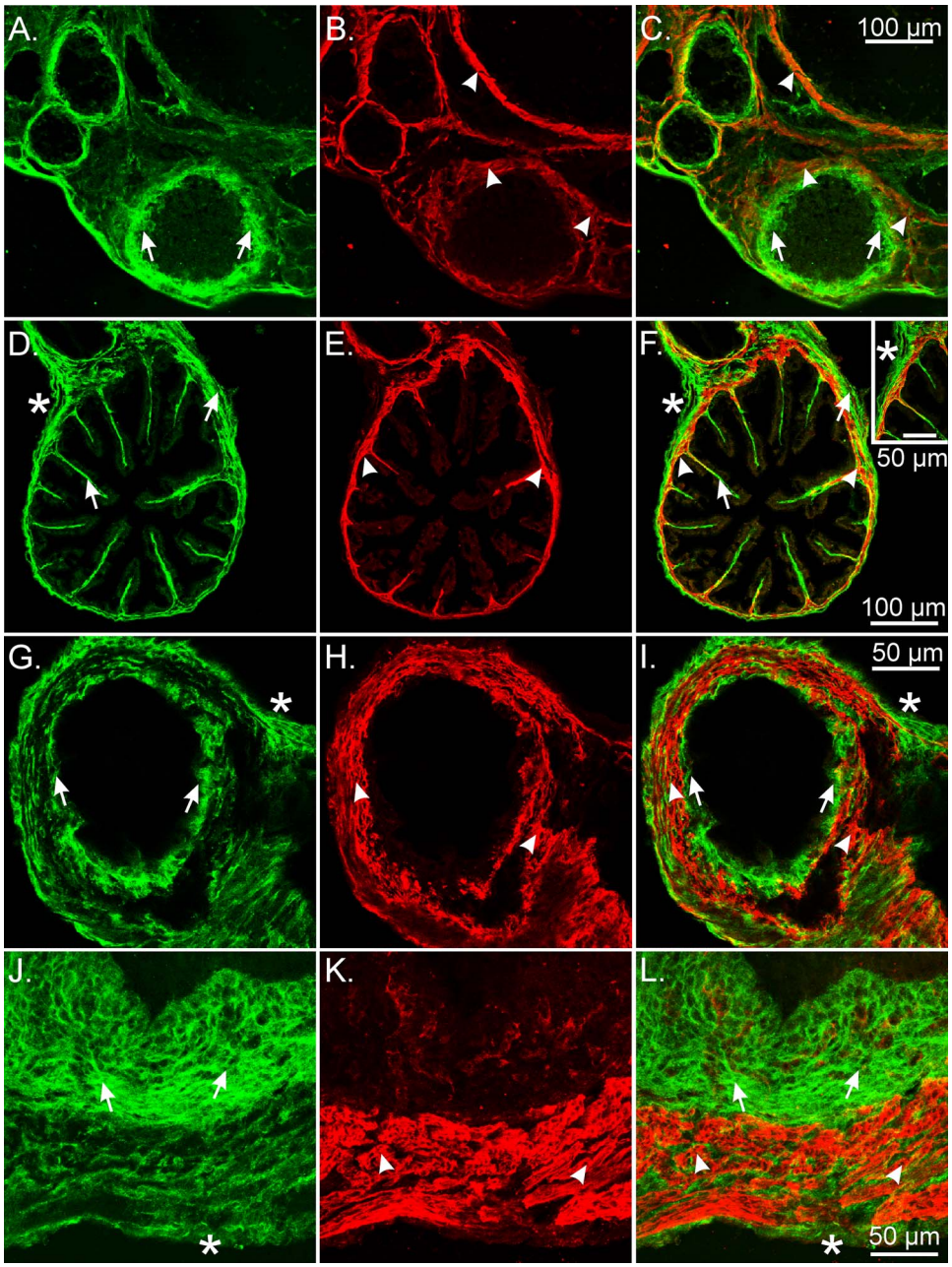

FIG. 5. PDGFRα and smooth muscle myosin heavy chain labeling in the mouse female reproductive tract. **A**–**C**) In ovaries, PDGFRα$^+$ cells (green; arrows) were distinct from SMCs (red; arrowheads). A distinct layer of Smmhc$^+$ SMCs that was several cells thick surrounded maturing follicles (**B** and **C**). Occasionally there was a thinning of the SMC layer towards the outer edges of larger follicles. **D**–**F**) In the ampulla, PDGFRα$^+$ cells were found in the serosal region of the ducts (*) and interspersed between SMCs within the myosalpinx. PDGFRα$^+$ cells (arrows) extended deeper into the lamina propria of the endosalpinx in the ampulla than SMCs did (arrowheads). Inset shows PDGFRα$^+$ cells in the ampulla. **G**–**I**) Isthmus PDGFRα$^+$ cells were present in similar locations as the ampulla but were more obvious in the myosalpinx because of the thicker muscle wall. Mucosal folds were reduced in the isthmus, and PDGFRα$^+$ cells were typically not observed. **J**–**L**) In the uterus, PDGFRα$^+$ cells (arrows) were densely distributed within the endometrial stroma, where Smmhc$^+$ SMCs were limited to blood vessels. PDGFRα$^+$ cells were also observed within the myometrium. This labeling was restricted to the interstitial spaces between SMCs (arrowheads). A layer of PDGFRα$^+$ cells was also observed on the serosa (*). Bars in **C**, **F**, **I**, and **L** represent their respective series of panels.

cells. PdgfAA was localized to oocyte and somatic cell clusters and within granulosa cells of follicles. PdgfB was localized to theca cells of secondary and antral follicles and was also apparent in the basement membrane between the granulosa and theca cell layers of secondary follicles. Prominent PdgfC labeling was present in cells of the theca layer of follicles [30]. PDGFRα$^+$ cells were reported to be distributed in primordial follicles, localized to either the oocyte or pregranulosa cells in the rat [30], and to theca cells and basal granulosa cells (weakly) in the pig [32], whereas PDGFRβ$^+$ cells were localized to cells surrounding primordial and primary follicles and in the thecal cells of follicles of rat and pig [30, 33]. The present study expands these studies to include a description of the cells expressing PDGFRα in mouse and NHPs. Within the corpus luteum, PDGFRα$^+$ cells were also localized to a population of luteal parenchymal cells, whereas PDGFRβ expression was localized to the luteal microvasculature [31]. Intraovarian injection of tyrphostin AG1295, an inhibitor of

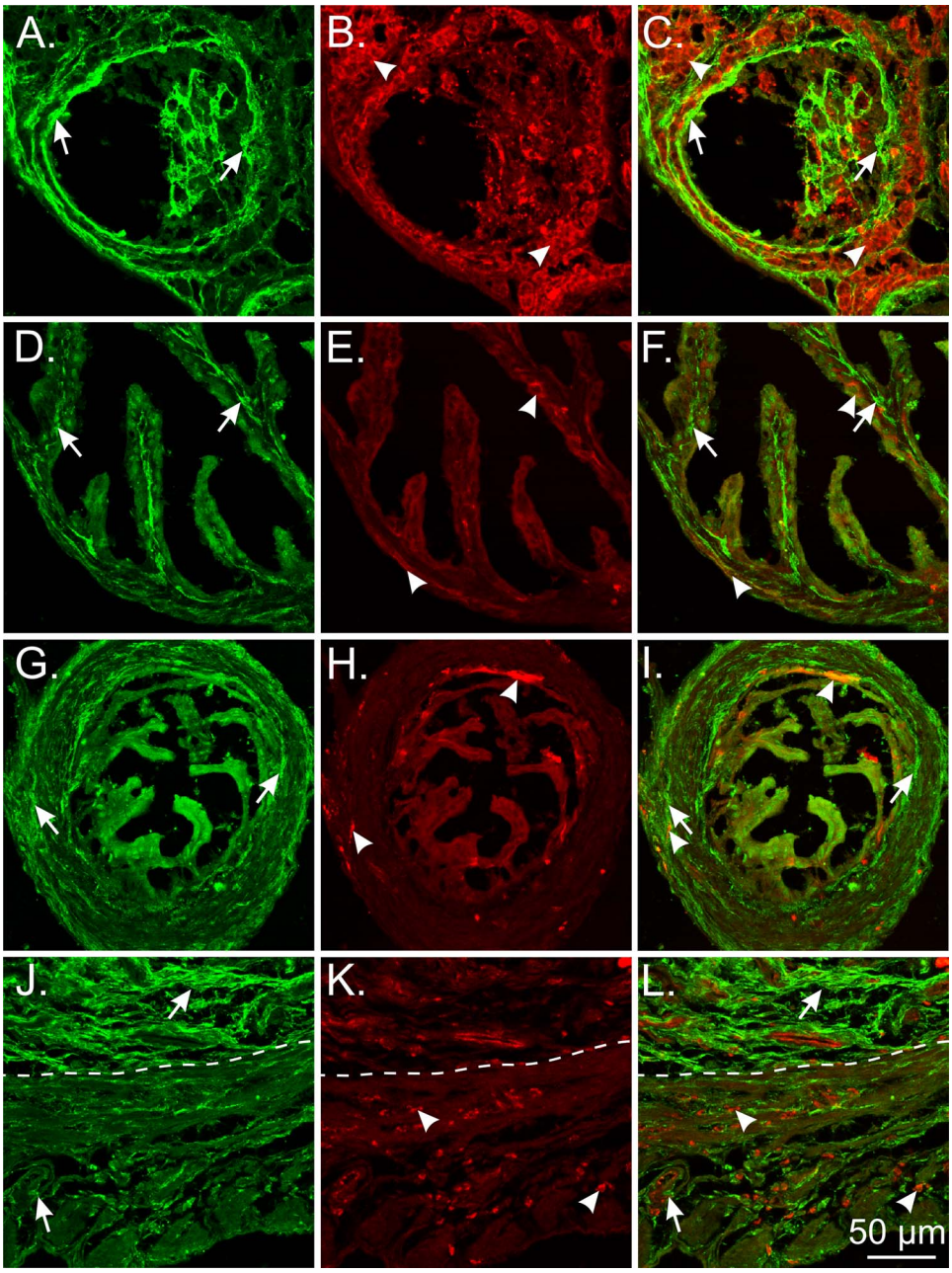

FIG. 6. Limited cellular colocalization of PDGFRα and vimentin in the mouse female reproductive tract. **A**–**C**) PDGFRα$^+$ cells (green; arrows) and vimentin$^+$ cells (red; arrowheads) in the ovary. Vimentin$^+$ cells surrounded follicles but were distinct from PDGFRα$^+$ cells. **D**–**F**) PDGFRα$^+$ cells (green; arrows) and vimentin$^+$ cells (red; arrowheads) in the ampulla region of the oviduct. Few vimentin$^+$ cells were located in the myosalpinx and endosalpinx. **G**–**I**) PDGFRα$^+$ and vimentin$^+$ cells in the isthmus region of the oviduct. There was a sparse distribution of vimentin$^+$ cells in the myosalpinx and endosalpinx. **J**–**L**) PDGFRα$^+$ cells and vimentin$^+$ cells in the uterus (myometrium and endometrium). Vimentin$^+$ cells were localized around smooth muscle bundles in the myometrium and interspersed between PDGFRα$^+$ cells in the endometrium and within the wall of blood vessels. The dotted line separates the endometrium (upper) from the myometrium (lower). Bar in **L** applies to all panels.

PDGF receptor activity, caused a significant decrease in the number of corpora lutea per treated ovary in comparison with the contralateral vehicle-injected control ovary. In addition, some of the treated ovaries displayed widespread hemorrhage throughout the entire ovary, indicating a possible role for PDGF receptor activity in the maintenance of the integrity of the ovarian vasculature [31].

To determine whether PDGFRα$^+$ cells represented a distinct population of interstitial cell, we performed double-label immunohistochemistry using antibodies against smooth muscle myosin II heavy chain (Smmhc), a specific marker for SMCs [34] and c-Kit, to identify ICCs, which are the pacemaker cells in the oviduct [26, 35]. PDGFRα$^+$ cells did not express considerable Smmhc, supported by a significant fold decrease in *Myh11* expression in oviduct and uterus (Table 3), suggesting they were distinct from SMC in these organs. This finding is not totally conclusive that PDGFRα$^+$ cells do not express Smmhc or that SMCs do not express PDGFRα, just that the protein was below the level of detection using immunohistochemistry. Interestingly, a distinct layer of SMCs was observed to surround follicles, and in some sections there was an apparent thinning of the smooth muscle layer towards

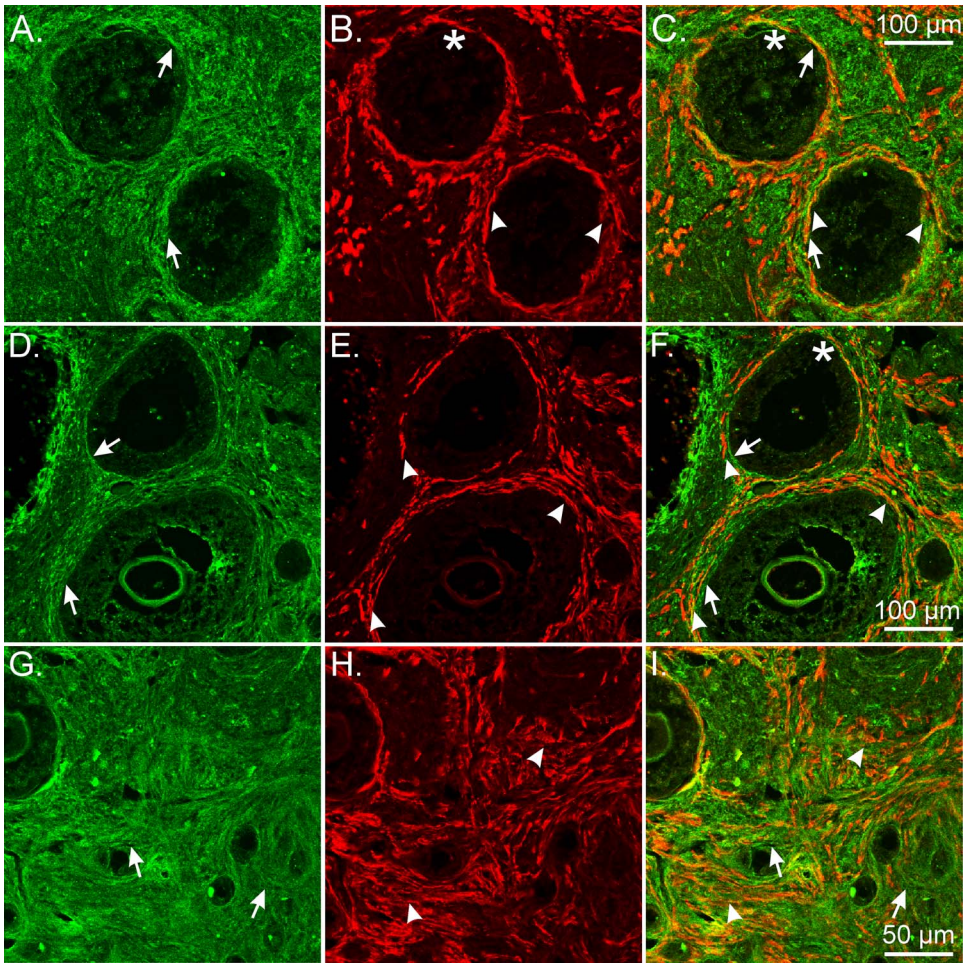

FIG. 7. PDGFRα$^+$ and Smmhc$^+$ cells represent distinct populations of cells in the NHP ovary. **A**, **D**, and **G**) In monkey ovary, PDGFRα$^+$ cells were distributed within the theca externa and interna (green; arrows). PDGFRα$^+$ cells were immunonegative for Smmhc, providing evidence they were distinct from SMCs. **B** and **C**) Similar to that observed in mouse, Smmhc$^+$ SMCs surrounded follicles (arrowheads; **B** and **E**, and **C** and **F**). *Asymmetric distribution of SMC layers around follicles that is thinner in this area. **G**–**I**) At higher power the complicated morphological interrelationship between PDGFRα$^+$ cells (arrows) and SMCs (arrowheads) is revealed. Bars in **C**, **F**, and **I** represent their respective series of panels.

their outer edges. The role of smooth muscle contraction in ovulation has received little attention; however, it has been suggested that follicular smooth muscle contractions cause the formation of rupture sites and are necessary for ovulation [23, 24]. In the ovary, endothelin-2 (EDN2) is exclusively and transiently expressed in the granulosa cells immediately before ovulation. Administration of EDN2 to ovarian tissues caused rapid contraction of follicular SMC, and treatment with the END2 receptor antagonist tezosentan before ovulation substantially decreased gonadotropin-induced superovulation. From these studies it was concluded that EDN2-induced follicular rupture occurred by constriction of periovulatory follicular smooth muscle [25]. In the oviduct and uterus, PDGFRα$^+$ cells also did not express c-Kit, a marker for pacemaker cells in visceral muscles, and this was also generally supported by fold decreases of gene expression that showed lower levels of *Kit* in sorted PDGFRα$^+$ cells compared with the total cellular population. In the ovary, it has been shown previously that Kit ligand (stem cell factor) is synthesized by granulosa cells [36, 37] and binds to Kit expressed by oocytes, facilitating the development of the oocyte and stromal cells. Theca cells also express Kit, and their signaling via stem cell factor promotes the formation and proliferation of these cells [38].

PDGFRα labeling has recently been used to identify a specialized interstitial cell in the GI tracts of rodents [12–14, 39–41], and more recently in humans [42]. These cells, previously known only as ''fibroblast-like'' cells, are closely apposed to enteric motor neurons in the tunica muscularis of the GI tract [12–14, 18, 39–41]. Expression of key receptor and effector proteins raised the possibility that they could be involved in motor neurotransmission, and it was shown that they respond to purine neurotransmitters with robust hyperpolarization responses due to the activation of small conductance calcium-activated potassium channel (SK3) channels and the development of outward current [14]. These cells are now considered a primary target for purinergic inhibitory neurotransmission in the GI tract. An additional population of PDGFRα$^+$ cells exists adjacent to the basolateral surfaces of epithelial cells of the mucosal layers in mouse and humans [42]. The functions of PDGFRα$^+$ cells in the mucosa are not yet determined.

PDGFRα$^+$ cells have also been investigated in mouse, guinea pig, and human bladders. PDGFRα$^+$ cells have been identified in the suburothelium and lamina propria of the bladder mucosa, as well as within detrusor SMCs [15, 17]. These cells were spindle or stellate shaped and formed a loose network. Their close apposition to intramural nerves [15, 17], as well as their robust expression of the purinergic P2Y1

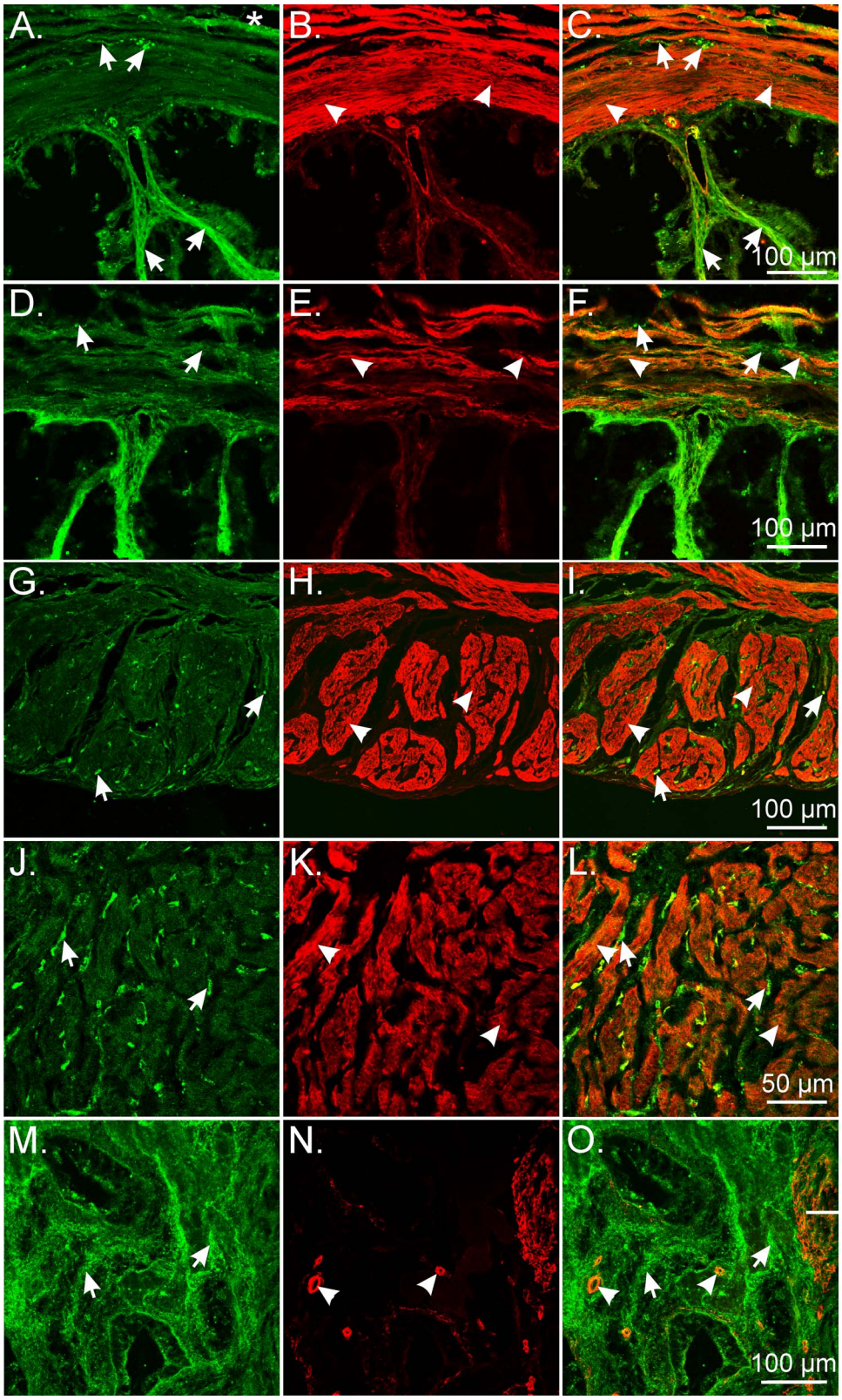

FIG. 8. Double labeling of PDGFRα and Smmhc reveal distinct populations of cells in the NHP oviduct and uterus. **A**–**F**) In the monkey oviduct, PDGFRα^{+} cells (green; arrows) were located along the serosa (*), within the myosalpinx (arrows), and deeper in the endosalpinx and mucosal folds (arrows) compared with Smmhc^{+} SMCs (red; arrowheads), which were primarily localized in the myosalpinx and blood vessels. **G**–**L**) In the monkey myometrium, PDGFRα^{+} cells (arrows) were located around muscle bundles (arrowheads) and within septa that separated these bundles. **J**–**L**) At higher power, distinct populations of PDGFRα^{+} and Smmhc^{+} SMCs are readily distinguished. PDGFRα^{+} cells within the myometrium (green; arrows) are interspersed between and surrounding smooth muscle bundles (red; arrowheads). **M**–**O**) In the uterine endometrium, PDGFRα^{+} cells formed a meshlike network of cells (arrows) that were distinct from the sparse Smmhc^{+} SMCs (arrowheads) that were localized to blood vessels. Bars in **C**, **F**, **I**, **L**, and **O** represent their respective series of panels.

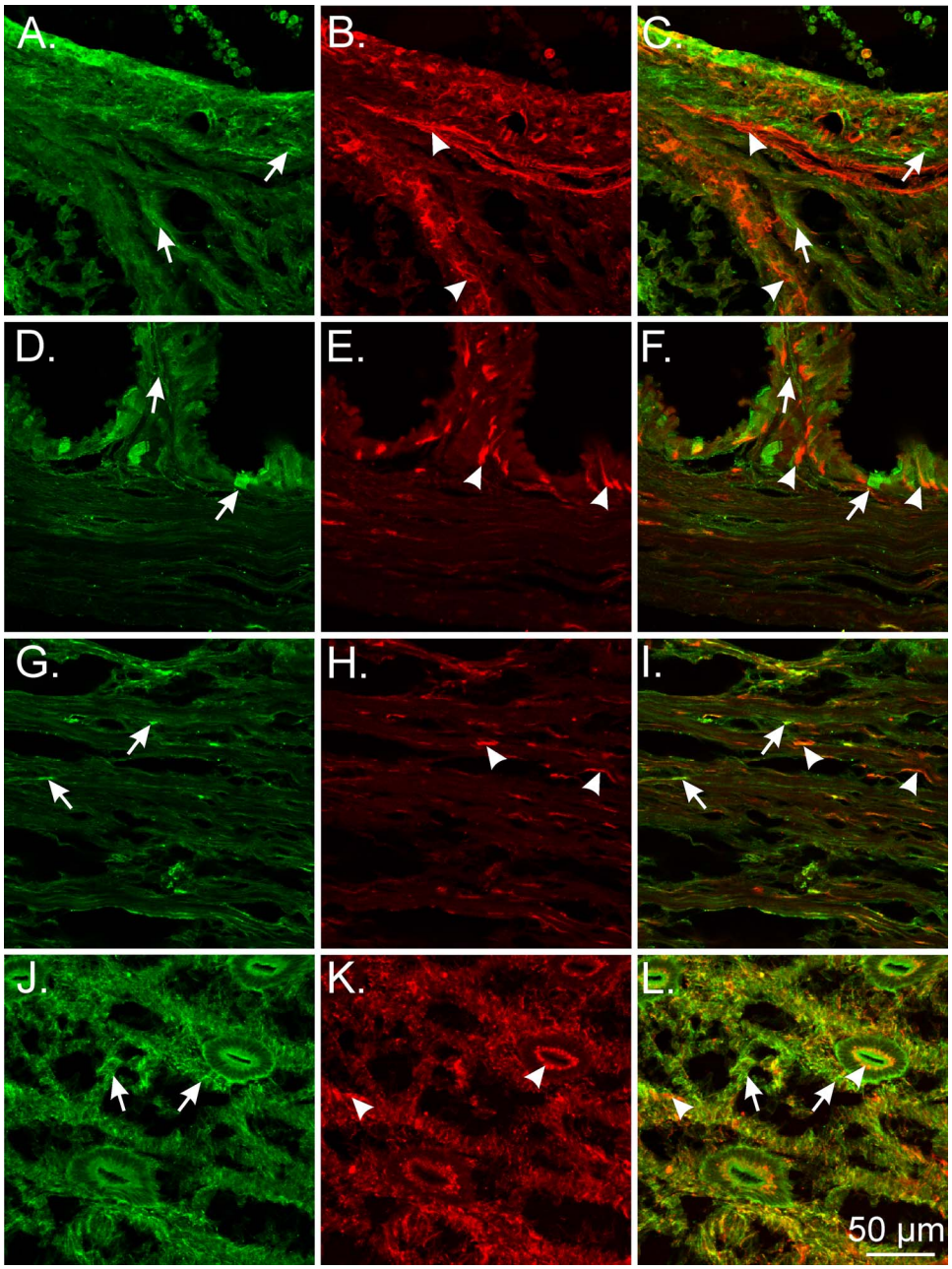

FIG. 9. Minimal cellular colocalization of PDGFRα and vimentin in the NHP female reproductive tract. **A**–**C**) PDGFRα$^+$ cells (green; arrows) and vimentin$^+$ cells (red; arrowheads) in the ovary. Vimentin$^+$ cells surrounded follicles and occasionally were located within the theca. **D**–**F**) PDGFRα$^+$ and vimentin$^+$ cells in the oviduct. Vimentin$^+$ cells were predominantly located within the endosalpinx with occasional cells in the myosalpinx. **G**–**I**) Vimentin$^+$ cells were widely distributed between and within smooth muscle bundles of the myometrium. **J**–**L**) PDGFRα$^+$ and vimentin$^+$ cells in the endometrium of the uterus. Vimentin$^+$ cells were within the stroma and surrounded endometrial glands. In the uterine endometrium, cellular colocalization of PDGFRα and vimentin was seen to exist in the monkey female reproductive tract. Bar in **L** applies to all panels.

receptor and SK3 channels [16], suggested involvement in purinergic neuroeffector responses [43]. Interestingly, some PDGFRα$^+$ cells in the bladder were reported to be vimentin and Kit positive, suggesting possible diversity in this type of interstitial cell in bladder and GI muscles [17]. Although the functional role(s) of PDGFRα$^+$ cells in the female reproductive tract remains unknown, by analogy to other visceral smooth muscle tissues these cells may provide important functions, such as neurotransduction and stabilization of excitability during stretch (filling) of the tissues. For example, if similar ionic conductances and mechanisms are identified in reproductive tract PDGFRα$^+$ cells, it is possible that these cells could be involved in the stabilization of uterine excitability as the fetus grows. The diverse distribution of these cells throughout the reproductive tract suggests many potential roles for these cells in the physiology of reproduction, and it will take some time to investigate their functional roles.

We took advantage of the expression of eGFP in the nuclei of *Pdgfra*$^+$ cells in *Pdgfra*$^{tm11\ (EGFP)Sor}$/J mice. Isolation of cells by enzymatic dispersion and subsequent purification of cells by FACS allowed cell-specific expression analysis on these unique populations of cells. The initial gene expression studies showed that cells were purified to a large extent, as

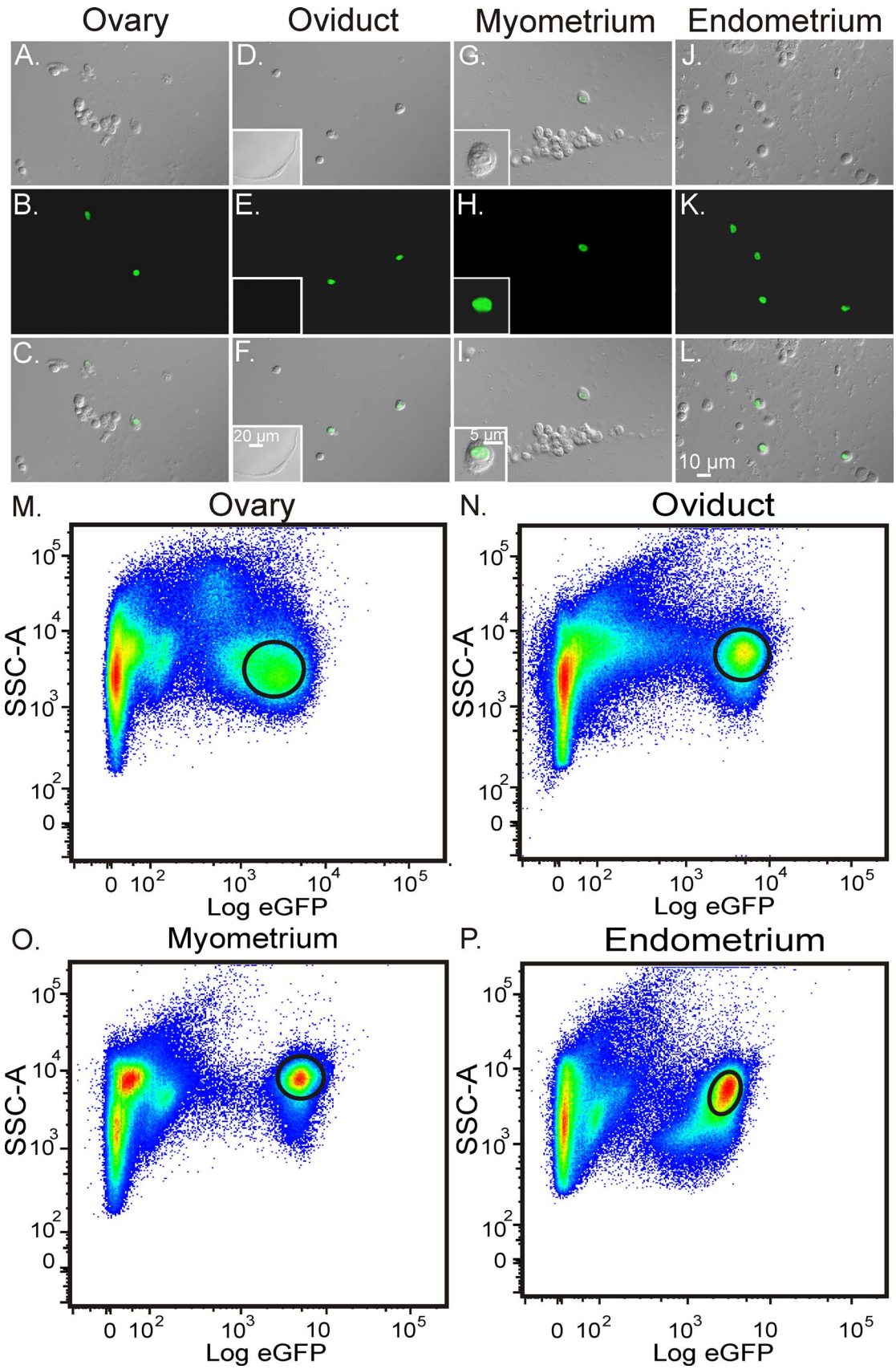

FIG. 10. Isolation and purification of PDGFRα^{+} cells within in the female reproductive tract. **A**–**L**) Enzymatically dispersed cells identified using DIC and confocal imaging prior to FACS sorting. **A**–**C**, Ovary; **D**–**F**, oviduct, **G**–**I**, uterine myometrium; and **J**–**L**, uterine endometrium. Fluorescence revealed nuclear labeling of eGFP in PDGFRα cells following enzymatic dispersion (**B**, **E**, **H**, and **K**; inset in **I**). **C**, **F**, **I**, and **L**) Smooth muscle cells were eGFP negative (inset in **F**). **M**–**P**) Enriched populations of eGFP-expressing PDGFRα^{+} cells following FACS. Graphs represent side scatter (SSC-A) as an indication of cellular granularity and complexity plotted against relative eGFP expression. Gates on each plot represent enriched eGFP^{+} cell populations sorted for molecular analysis. Note that there appear to be multiple subpopulations of PDGFRα^{+} cells in each tissue based on eGFP expression. Bar in **L** represents **A**–**L**.

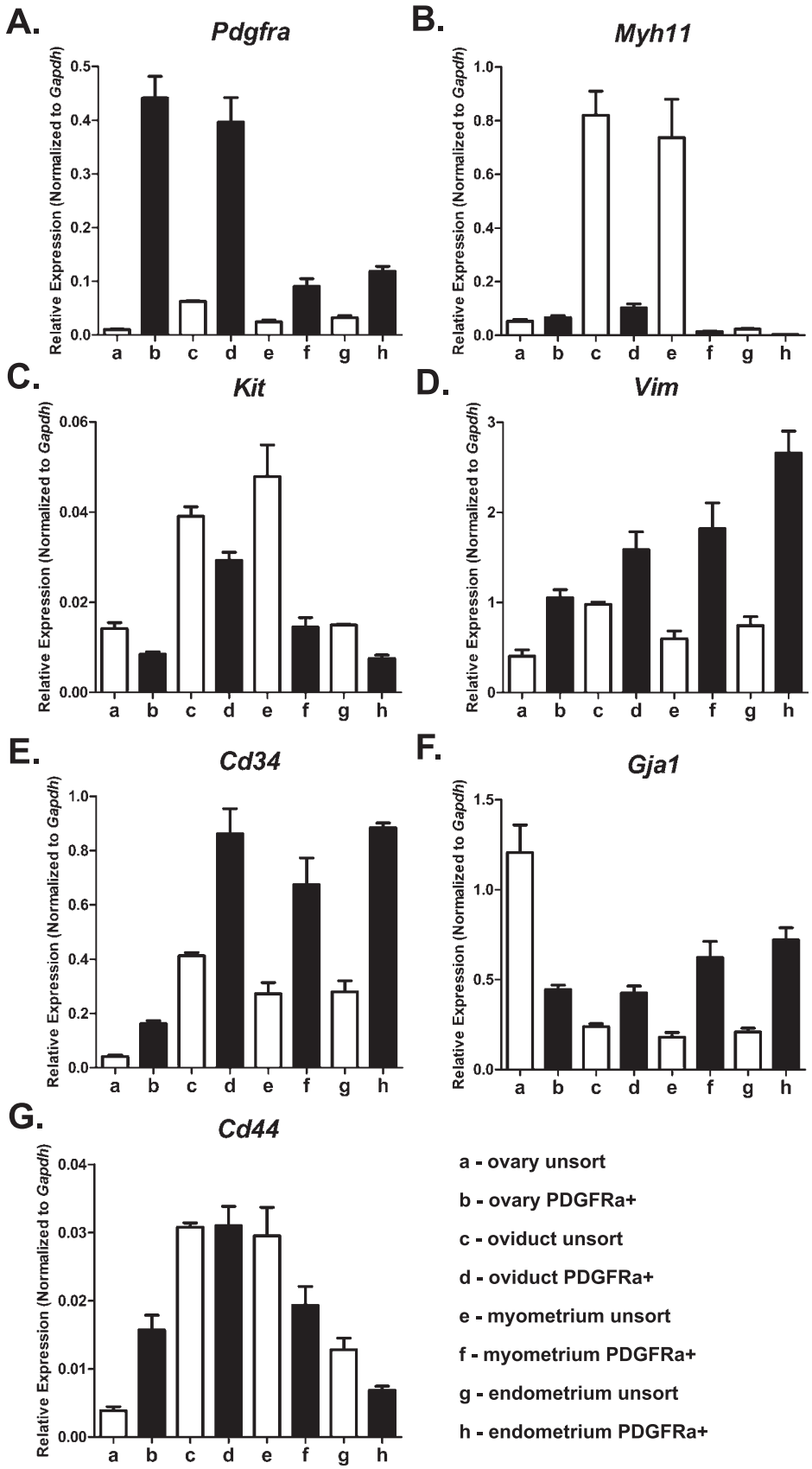

FIG. 11. Expression profiles of genes defining cellular phenotype in PDGFRα^+ cells. *Pdgfra* (PDGFRα^+ cells; **A**), *Myhll* (smooth muscle myosin; **B**), *Kit* (ICCs, pacemaker cells; **C**), *Vim* (vimentin, fibroblast-like cells; **D**), *Gja1* (gap junction alpha-1 protein or connexin 43; **E**), *Cd34* (mesenchymal stem cell marker; **F**), and *Cd44* (cell-cell integration, cell adhesion and migration, stem cell marker; **G**). Normalized values and SDs were calculated in differences of relative gene expression from four dilutions of technical duplicates of reproductive organs from each animal. The data are shown as averages and SDs of triplicate samples (n = 3).

TABLE 3. Fold changes of genes between sorted PDGFRα^+ cells and unsorted cells from different organs of the female reproductive tract.

Gene	Ovary	*P* value[a]	Oviduct	*P* value[a]	Myometrium	*P* value[a]	Endometrium	*P* value[a]
Pdgfra	43.6785	0.002**	6.3340	0.006**	3.7463	0.012*	3.6882	0.001**
Myh11	1.2599	0.095	−8.0398	0.004**	−53.0666	0.013*	−11.3120	0.040*
Kit	−1.6649	0.049*	−1.3320	0.050*	−3.3027	0.010**	−1.9811	0.025*
Ano1[b]	0.0000	0.000	0.000	0.000	0.0000	0.000	0.0000	0.000
Kcnn3	36.5789	0.001**	5.6925	0.005**	4.3813	0.008**	2.2204	0.009**
P2ry1	31.7300	0.005**	6.8228	0.005**	3.1081	0.017*	2.1209	0.002**
Vim	2.5971	0.007**	1.6220	0.043*	3.0378	0.012*	3.5800	0.002**
Fos	11.0327	0.001**	1.0884	0.305	1.6437	0.024*	−2.0309	0.010**
Gja1	−2.7187	0.011*	1.7804	0.027*	3.4477	0.009**	3.4559	0.003**
Cd34	3.8818	0.001**	2.0860	0.013*	2.4741	0.010**	3.1511	0.000**
Cd44	4.0626	0.008**	1.0067	0.917	−1.5281	0.050*	−1.8595	0.018*

[a] *P* values were rounded to three decimal places. Genes with a fold change *P* value less than 0.05 (*) and less than 0.01 (**) between PDGFRα^+ sorted and unsorted cells are identified [51].
[b] 0 = *Ano1* was below detection in sorted PDGFR$^+$ cells.

indicated by a substantial increase in expression of PDGFRα versus levels in unsorted cells. We examined whether these cells have the potential of forming gap junctions with one another to create an electrical syncytium, because of the dense meshlike network of PDGFRα^+ cells in the organs of the female reproductive tract. We found enrichment in transcripts for *Gja1*, which encodes connexin Cx43 in PDGFRα^+ cells, except in ovary, suggesting that these cells have the potential for gap junction formation.

PDGFRα^+ cells also expressed the early response transcription factor and proto-oncogene *Fos*. *Fos* has been shown to participate in a variety of cellular processes, including regulation of cell proliferation, differentiation, apoptosis, and transformation [44]. The deregulation of *Fos* has been linked to a variety of pathophysiological conditions, including oncogenic transformation [45]. *Fos* expression or amplification has been shown to occur in ovarian [46] and endometrial [47] carcinomas. Increased PDGFRα expression has been shown to occur in malignant ovarian and uterine

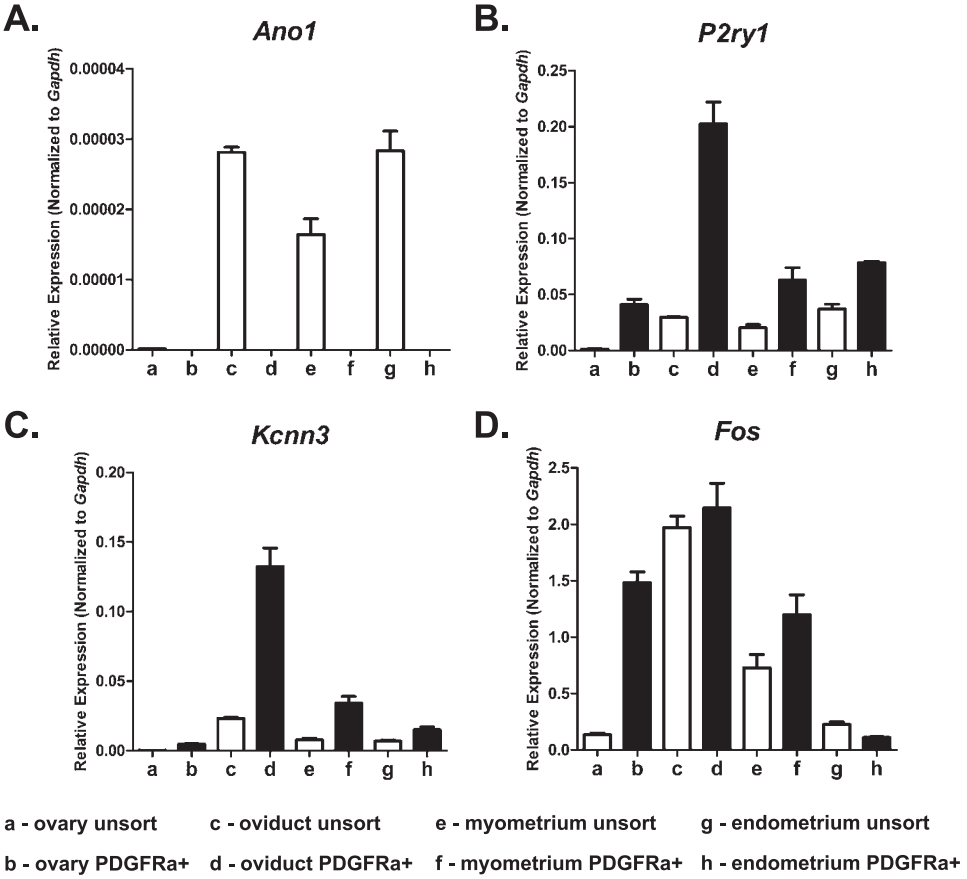

FIG. 12. Expression profiles of genes defining cellular function in PDGFRα^+ cells. *Ano1* (calcium-activated chloride conductance Anoctamin-1, also known as Tmem16a, involved in pacemaker activity; **A**), *P2ry1* (P2Y1 purine receptor; **B**), *Kcnn3* (K_{Ca}2.3 or SK3, small conductance calcium-activated potassium channel; **C**), and *Fos* (proto-oncogene; early response gene Fos; **D**). Normalized values and SDs were calculated in differences of relative gene expression from four dilutions of technical duplicates of reproductive organs from each animal. The data are shown as averages and SDs of triplicate samples (n = 3).

carcinomas, and increased PDGFRα expression is associated with significantly poorer overall survival in patients with these cancers [48]. PDGF signaling has been reported to cause upregulation of *Fos* [49, 50]. It is possible that mutations in PDGFRα could lead to an increase in *Fos* expression that might promote cellular oncogenesis, especially in ovarian tissues.

In summary, we used a novel mouse model that expresses eGFP in the nuclei of PDGFRα$^+$ cells. We investigated the expression of this new class of interstitial cell in the female reproductive tract and found these cells densely distributed in the muscle and mucosal tissues of ovary, oviduct, and uterus of both mice and monkeys. We used eGFP labeling to isolate and purify PDGFRα$^+$ cells by FACS and performed molecular characterizations of gene expression in cells from different reproductive organs and regions of organs. Differential expression of specific genes in PDGFRα$^+$ cells from different regions suggests diversity of functions between populations of cells. Large-scale determinations of gene expression and fate mapping will be performed in future studies to determine whether these cells change during the reproductive cycle, infections, and pregnancy. We may also be able to learn whether these cells serve as a source of cells that are transformed in malignancies originating in female reproductive organs.

REFERENCES

1. Thibault C, Levasseur MC. Ovulation. Hum Reprod 1988; 3:513–523.
2. Sánchez F, Smitz J. Molecular control of oogenesis. Biochim Biophys Acta 2012; 1822:1896–1912.
3. Canipari R, Cellini V, Cecconi S. The ovary feels fine when paracrine and autocrine networks cooperate with gonadotropins in the regulation of folliculogenesis. Curr Pharm Des 2012; 18:245–255.
4. Croxatto HB. Physiology of gamete and embryo transport through the fallopian tube. Reprod Biomed Online 2002;4:160–169.
5. Coy P, García-Vázquez FA, Visconti PE, Avilés M. Roles of the oviduct in mammalian fertilization. Reproduction 2012; 144:649–660.
6. Bazer FW, Spencer TE, Johnson GA, Burghardt RC. Uterine receptivity to implantation of blastocysts in mammals. Front Biosci (Schol Ed) 2011; 3: 745–767.
7. Smith R. Parturition. N Engl J Med 2007; 356:271–283.
8. Challis JR, Lye SJ. Parturition. Oxf Rev Reprod Biol 1986; 8:61–129.
9. Smith R, Van Helden D, Hirst J, Zakar T, Read M, Chan EC, Palliser H, Grammatopoulos D, Nicholson R, Parkington HC. Pathological interactions with the timing of birth and uterine activation. Aust N Z J Obstet Gynaecol 2007; 47:430–437.
10. Sanders KM, Ward SM, Koh SD. Interstitial cells: regulators of smooth muscle function. Physiol Rev 2014; 94:859–907.
11. Komuro T. Re-evaluation of fibroblasts and fibroblast-like cells. Anat Embryol (Berl) 1990; 182:103–112.
12. Iino S, Horiguchi K, Horiguchi S, Nojyo Y. c-Kit-negative fibroblast-like cells express platelet-derived growth factor receptor alpha in the murine gastrointestinal musculature. Histochem Cell Biol 2009; 131:691–702.
13. Iino S, Nojyo Y. Immunohistochemical demonstration of c-Kit-negative fibroblast-like cells in murine gastrointestinal musculature. Arch Histol Cytol 2009; 72:107–115.
14. Kurahashi M, Zheng H, Dwyer L, Ward SM, Don Koh S, Sanders KM. A functional role for the 'fibroblast-like cells' in gastrointestinal smooth muscles. J Physiol 2011; 589(pt 3):697–710.
15. Koh BH, Roy R, Hollywood MA, Thornbury KD, McHale NG, Sergeant GP, Hatton WJ, Ward SM, Sanders KM, Koh SD. Platelet-derived growth factor receptor-α cells in mouse urinary bladder: a new class of interstitial cells. J Cell Mol Med 2012; 16:691–700.
16. Lee H, Koh BH, Peri LE, Sanders KM, Koh SD. Functional expression of SK channels in murine detrusor PDGFR+ cells. J Physiol 2013; 591(pt 2): 503–513.
17. Monaghan KP, Johnston L, McCloskey KD. Identification of PDGFRα positive populations of interstitial cells in human and guinea pig bladders. J Urol 2012; 188:639–647.
18. Kurahashi M, Nakano Y, Peri LE, Townsend JB, Ward SM, Sanders KM. A novel population of subepithelial platelet-derived growth factor receptor α-positive cells in the mouse and human colon. Am J Physiol Gastrointest Liver Physiol 2013; 304:G823–G834.
19. Hamilton TG, Klinghoffer RA, Corrin PD, Soriano P. Evolutionary divergence of platelet-derived growth factor alpha receptor signaling mechanisms. Mol Cell Biol 2003; 23:4013–4025.
20. Zhu MH, Kim TW, Ro S, Yan W, Ward SM, Koh SD, Sanders KMA. Ca(2+)-activated Cl(-) conductance in interstitial cells of Cajal linked to slow wave currents and pacemaker activity. J Physiol 2009; 587(pt 20): 4905–4918.
21. Kurahashi M, Niwa Y, Cheng J, Ohsaki Y, Fujita A, Goto H, Fujimoto T, Torihashi S. Platelet-derived growth factor signals play critical roles in differentiation of longitudinal smooth muscle cells in mouse embryonic gut. Neurogastroenterol Motil 2008; 20:521–531.
22. Donovan J, Abraham D, Norman J. Platelet-derived growth factor signaling in mesenchymal cells. Front Biosci (Landmark Ed) 2013; 18: 106–119.
23. Schroeder PC, Talbot P. Intrafollicular pressure decreases in hamster preovulatory follicles during smooth muscle cell contraction in vitro. J Exp Zool 1982; 224:417–426.
24. Talbot P, Chacon RS. In vitro ovulation of hamster oocytes depends on contraction of follicular smooth muscle cells. J Exp Zool 1982; 224: 409–415.
25. Ko C, Gieske MC, Al-Alem L, Hahn Y, Su W, Gong MC, Iglarz M, Koo Y. Endothelin-2 in ovarian follicle rupture. Endocrinology 2006; 147: 1770–1779.
26. Dixon RE, Hwang SJ, Hennig GW, Ramsey KH, Schripsema JH, Sanders KM, Ward SM. Chlamydia infection causes loss of pacemaker cells and inhibits oocyte transport in the mouse oviduct. Biol Reprod 2009; 80: 665–673.
27. Torihashi S, Ward SM, Sanders KM. Development of c-Kit-positive cells and the onset of electrical rhythmicity in murine small intestine. Gastroenterology 1997; 112:144–155.
28. Gibbs RA, Rogers J, Katze MG, Bumgarner R, Weinstock GM, Mardis ER, Remington KA, Strausberg RL, Venter JC, Wilson RK, Batzer MA, Bustamante CD, et al; Rhesus Macaque Genome Sequencing and Analysis Consortium. Evolutionary and biomedical insights from the rhesus macaque genome. Science 2007; 316:222–234.
29. Hwang SJ, Blair PJ, Britton FC, O'Driscoll KE, Hennig G, Bayguinov YR, Rock JR, Harfe BD, Sanders KM, Ward SM. Expression of anoctamin 1/TMEM16A by interstitial cells of Cajal is fundamental for slow wave activity in gastrointestinal muscles. J Physiol 2009; 587(pt 20): 4887–4904.
30. Sleer LS, Taylor CC. Platelet-derived growth factors and receptors in the rat corpus luteum: localization and identification of an effect on luteogenesis. Biol Reprod 2007; 76:391–400.
31. Sleer LS, Taylor CC. Cell-type localization of platelet-derived growth factors and receptors in the postnatal rat ovary and follicle. Biol Reprod 2007; 76:379–390.
32. Okamura Y, Myoumoto A, Manabe N, Tanaka N, Okamura H, Fukumoto M. Protein tyrosine kinase expression in the porcine ovary. Mol Hum Reprod 2001; 7:723–729.
33. Taylor CC. Platelet-derived growth factor activates porcine thecal cell phosphatidylinositol-3-kinase-Akt/PKB and ras-extracellular signal-regulated kinase-1/2 kinase signaling pathways via the platelet-derived growth factor-beta receptor. Endocrinology 2000; 141:1545–1553.
34. Miano JM. Vascular smooth muscle cell differentiation-2010. J Biomed Res 2010; 24:169–180.
35. Shafik A, Shafik AA, El Sibai O, Shafik IA. Specialized pacemaking cells in the human Fallopian tube. Mol Hum Reprod 2005; 11:503–505.
36. Motro B, van der Kooy D, Rossant J, Reith A, Bernstein A. Contiguous patterns of c-kit and steel expression: analysis of mutations at the W and Sl loci. Development 1991; 113:1207–1221.
37. Manova K, Huang EJ, Angeles M, De Leon V, Sanchez S, Pronovost SM, Besmer P, Bachvarova RF. The expression pattern of the c-kit ligand in gonads of mice supports a role for the c-kit receptor in oocyte growth and in proliferation of spermatogonia. Dev Biol 1993; 157:85–99.
38. Parrott JA, Skinner MK. Direct actions of kit-ligand on theca cell growth and differentiation during follicle development. Endocrinology 1997; 138: 3819–3827.
39. Cobine CA, Hennig GW, Kurahashi M, Sanders KM, Ward SM, Keef KD. Relationship between interstitial cells of Cajal, fibroblast-like cells and inhibitory motor nerves in the internal anal sphincter. Cell Tissue Res 2011; 344:17–30.
40. Baker SA, Hennig GW, Salter AK, Kurahashi M, Ward SM, Sanders KM. Distribution and Ca(2+) signalling of fibroblast-like (PDGFR(+)) cells in the murine gastric fundus. J Physiol 2013; 591(pt 24):6193–6208.
41. Hall KA, Ward SM, Cobine CA, Keef KD. Spatial organization and

coordination of slow waves in the mouse anorectum. J Physiol 2014; 592: 3813–3829.
42. Kurahashi M, Nakano Y, Hennig GW, Ward SM, Sanders KM. Platelet-derived growth factor receptor α-positive cells in the tunica muscularis of human colon. J Cell Mol Med 2012; 16:1397–1404.
43. Lee H, Koh BH, Peri LE, Sanders KM, Koh SD. Purinergic inhibitory regulation of murine detrusor muscles mediated by PDGFRα^+ interstitial cells. J Physiol 2014; 592(pt 6):1283–1293.
44. Durchdewald M, Angel P, Hess J. The transcription factor Fos: a Janus-type regulator in health and disease. Histol Histopathol 2009; 24: 1451–1461.
45. Ordway JM, Fenster SD, Ruan H, Curran T. A transcriptome map of cellular transformation by the fos oncogene. Mol Cancer 2005; 4:19.
46. Tsuda H, Birrer MJ, Ito YM, Ohashi Y, Lin M, Lee C, Wong WH, Rao PH, Lau CC, Berkowitz RS, Wong KK, Mok SC. Identification of DNA copy number changes in microdissected serous ovarian cancer tissue using a cDNA microarray platform. Cancer Genet Cytogenet 2004; 155:97–107.
47. Bamberger AM, Milde-Langosch K, Rössing E, Goemann C, Löning T. Expression pattern of the AP-1 family in endometrial cancer: correlations with cell cycle regulators. J Cancer Res Clin Oncol 2001; 127:545–550.
48. Henriksen R, Funa K, Wilander E, Bäckström T, Ridderheim M, Oberg K. Expression and prognostic significance of platelet-derived growth factor and its receptors in epithelial ovarian neoplasms. Cancer Res 1993; 53: 4550–4554.
49. Black PM, Carroll R, Glowacka D, Riley K, Dashner K. Platelet-derived growth factor expression and stimulation in human meningiomas. J Neurosurg 1994; 81:388–393.
50. Chui CM, Li K, Yang M, Chuen CK, Fok TF, Li CK, Yuen PM. Platelet-derived growth factor up-regulates the expression of transcription factors NF-E2, GATA-1 and c-Fos in megakaryocytic cell lines. Cytokine 2003; 21:51–64.
51. Karlen Y, McNair A, Perseguers S, Mazza C, Mermod N. Statistical significance of quantitative PCR. BMC Bioinformatics 2007; 8:131–147.